

Electronic Supporting Information (ESI) for

**Detection of TNP and Sulfite Ion in Aqueous Medium by Pyrazinium-based Chemosensor**

Pragya,<sup>a</sup> Krishnan Rangan,<sup>b</sup> Bharti Khungar<sup>a\*</sup>

<sup>a</sup>Department of Chemistry, Birla Institute of Technology and Science Pilani, Pilani Campus, Pilani, Rajasthan, 333031, India

<sup>b</sup>Department of Chemistry, Birla Institute of Technology and Science Pilani, Hyderabad Campus, Secunderabad, Telangana, 500078, India  
*E-mail address:* [bkhungar@pilani.bits-pilani.ac.in](mailto:bkhungar@pilani.bits-pilani.ac.in)

**Table of contents**

Fig. S1 <sup>1</sup>H NMR of **PPyz** in CDCl<sub>3</sub>

Fig. S2 <sup>13</sup>C NMR of **PPyz** in CDCl<sub>3</sub>

Fig. S3 HRMS of **PPyz**

Fig. S4 <sup>1</sup>H NMR of **BPPyz** in DMSO-d<sub>6</sub>

Fig. S5 <sup>13</sup>C NMR of **BPPyz** in DMSO-d<sub>6</sub>

Fig. S6 HRMS of **BPPyz**

Fig. S7 ORTEP diagram of **BPPyz**

Fig. S8 UV-visible and fluorescence spectra of **BPPyz**

Fig. S9 Solvent study of **BPPyz** ( $2 \times 10^{-5}$  M)

Fig. S10 Individual UV-visible spectra of **BPPyz**, **BPPyz-TNP** and TNP

Fig. S11 Comparison of percentage fluorescence quenching obtained on addition of TNP, 2,4-DNP and 4-NP to the solution of **BPPyz** in water ( $2 \times 10^{-5}$  M)

Fig. S12 Interference study of **BPPyz** toward TNP selectivity in the presence of (a) anions, (b) cations, and (c) organic analytes

Fig. S13 Effect of pH on **BPPyz**, **BPPyz + TNP** and **BPPyz + SO<sub>3</sub><sup>2-</sup>**

Fig. S14 Fluorescence spectra for **BPPyz** ( $2 \times 10^{-5}$  M) with different amounts of 2,4-DNP

Fig. S15 Fluorescence spectra for **BPPyz** ( $2 \times 10^{-5}$  M) with different amounts of 4-NP

Fig. S16 Calibration curve with error bar for calculating Detection Limit of TNP

Fig. S17 Stern-Volmer plot of **BPPyz** using TNP as a quencher ( $2 \times 10^{-5}$  M)

Fig. S18 Stern-Volmer plot of **BPPyz** using 2,4-DNP as a quencher ( $2 \times 10^{-5}$  M)

Fig. S19 Stern-Volmer plot of **BPPyz** using 4-NP as a quencher ( $2 \times 10^{-5}$  M)

Fig. S20 Spectral overlap of organic analytes and **BPPyz**

Fig. S21 Lifetime decay plot of **BPPyz**, **BPPyz-TNP** and **BPPyz-SO<sub>3</sub><sup>2-</sup>** complexes

Fig. S22 Inner filter effect correction of **BPPyz**

Fig. S23 Fluorescence spectra of **BPPyz** and **BPPyz** with TFA in aqueous medium

Fig. S24 <sup>1</sup>H NMR of **BPPyz-TNP** complex DMSO-*d*<sub>6</sub>

Fig. S25 HRMS of **BPPyz-TNP** complex

Fig. S26 HOMO-LUMO energy levels of **BPPyz** and organic analytes

Fig. S27 Stern–Volmer plot of **BPPyz** using SO<sub>3</sub><sup>2-</sup> as a quencher

Fig. S28 Job's Plot of **BPPyz** with SO<sub>3</sub><sup>2-</sup>

Fig. S29 Selectivity of **BPPyz** toward SO<sub>3</sub><sup>2-</sup> in the presence of anions

Fig. S30 Calibration curve with error bar for calculating Detection Limit of SO<sub>3</sub><sup>2-</sup>

Fig. S31 <sup>1</sup>H NMR of **BPPyz-SO<sub>3</sub><sup>2-</sup>** complex in DMSO-*d*<sub>6</sub>

Fig. S32 <sup>13</sup>C NMR of **BPPyz-SO<sub>3</sub><sup>2-</sup>** complex in DMSO-*d*<sub>6</sub>

Fig. S33 HRMS of **BPPyz-SO<sub>3</sub><sup>2-</sup>** complex

Fig. S34 Sketch of Photo light box for RGB analysis

Fig. S35 The ratio of RGB (a) R/(R+G+B) (b) G/(R+G+B) (c) B/(R+G+B) (d) R/G (e) R/B (f) G/B versus SO<sub>3</sub><sup>2-</sup> concentration in the range of 0 to 20.0 μM.

## List of tables

Table S1 Single-crystal XRD data and structure refinement of **BPPyz** and **BPPyz-TNP** complex

Table S2 Bond Lengths of **BPPyz**

Table S3 Bond Angles of **BPPyz**

Table S4 Bond Lengths of **BPPyz-TNP** complex

Table S5 Bond Angles of **BPPyz-TNP** complex

Table S6 A comparison of literature reported Chemosensors for TNP detection.

Table S7 A comparison of literature reported Chemosensors for SO<sub>3</sub><sup>2-</sup> detection

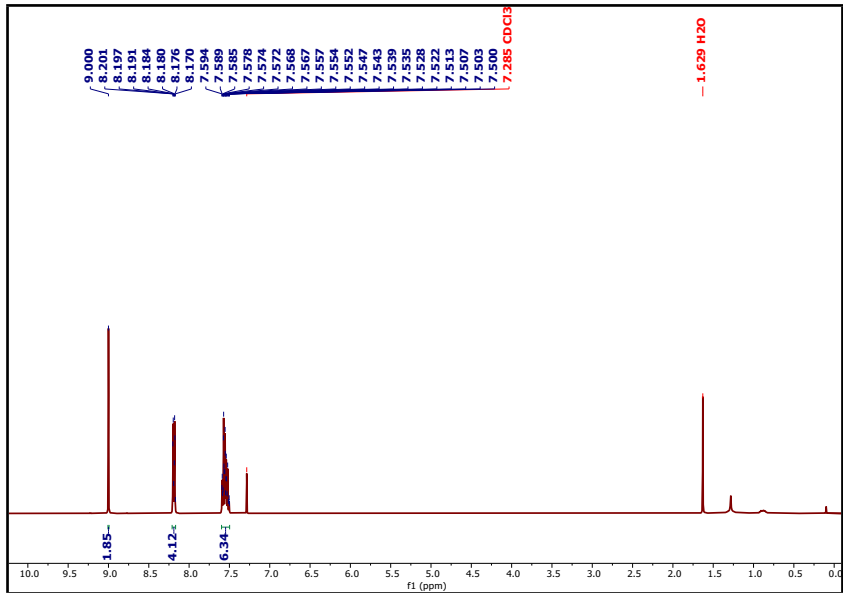


Fig. S1 <sup>1</sup>H NMR of PPyz in  $\text{CDCl}_3$

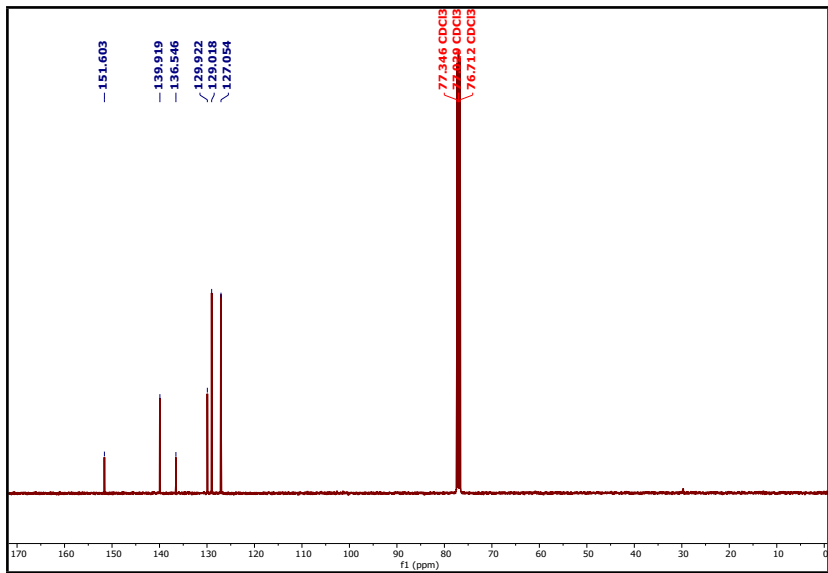


Fig. S2 <sup>13</sup>C NMR of PPyz in  $\text{CDCl}_3$

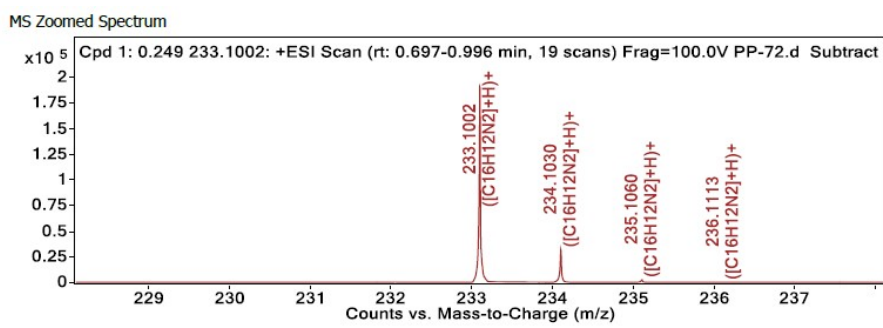


Fig. S3 HRMS of PPyz

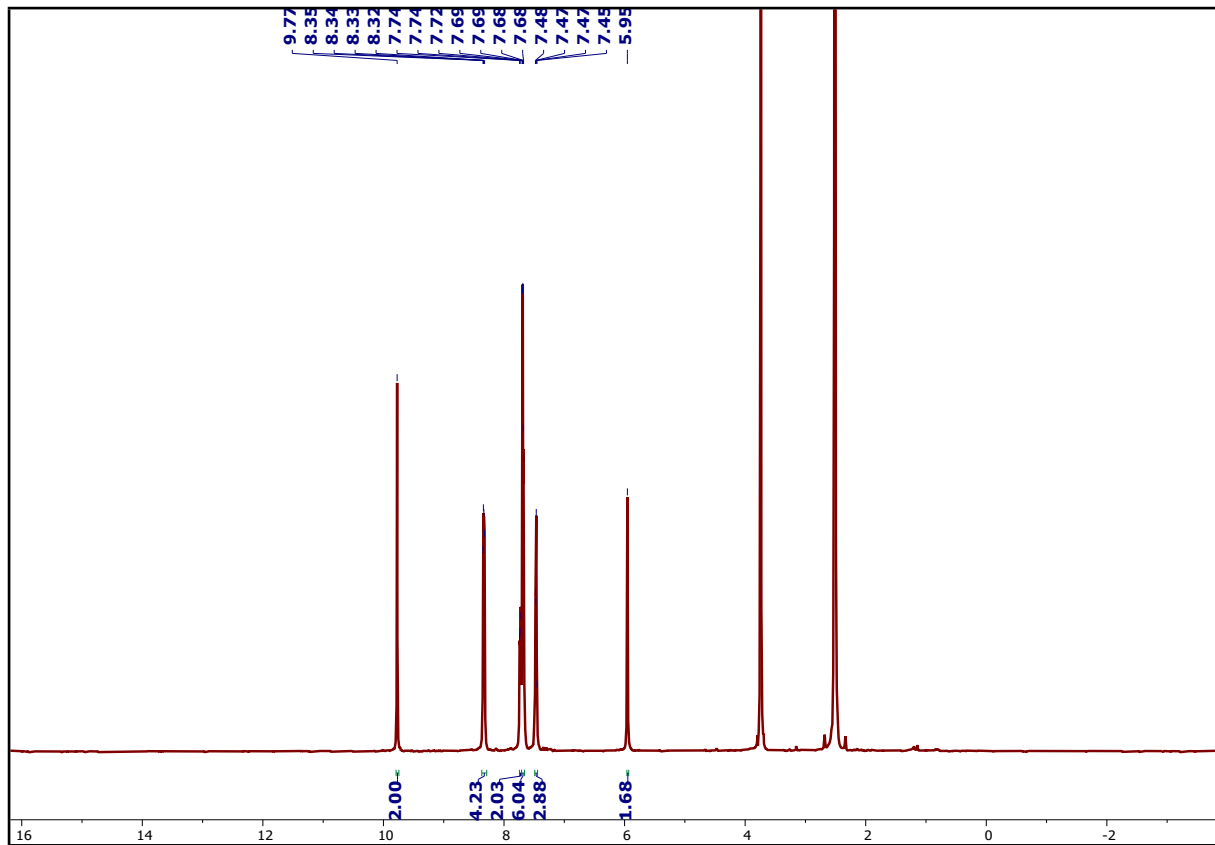


Fig. S4  $^1\text{H}$  NMR of BPPyz in  $\text{DMSO}-d_6$

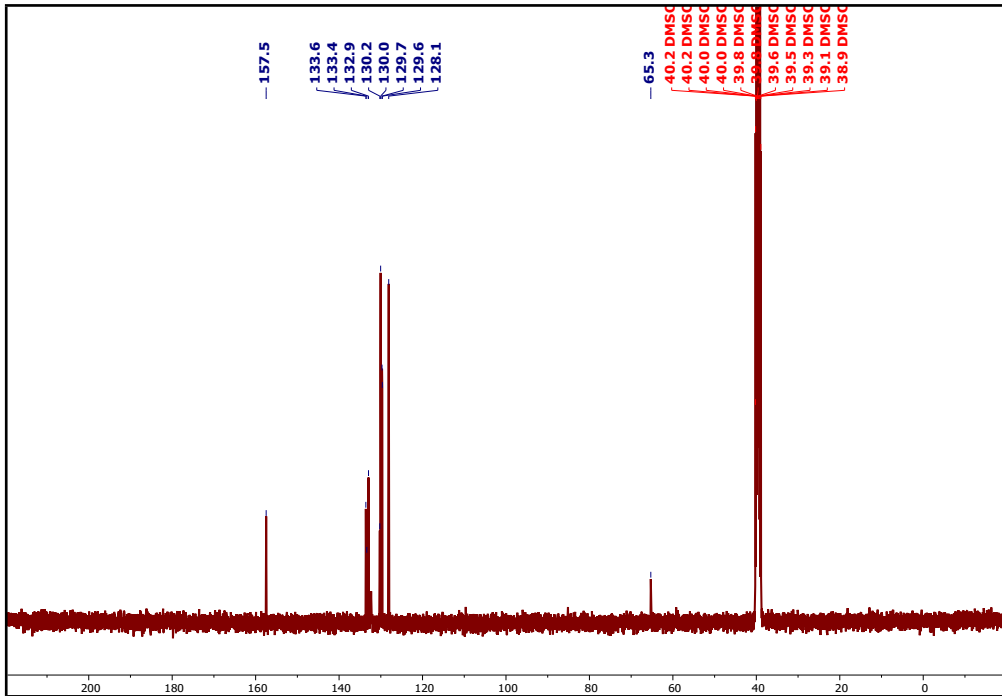


Fig. S5  $^{13}\text{C}$  NMR of BPPyz in  $\text{DMSO}-d_6$

MS Zoomed Spectrum

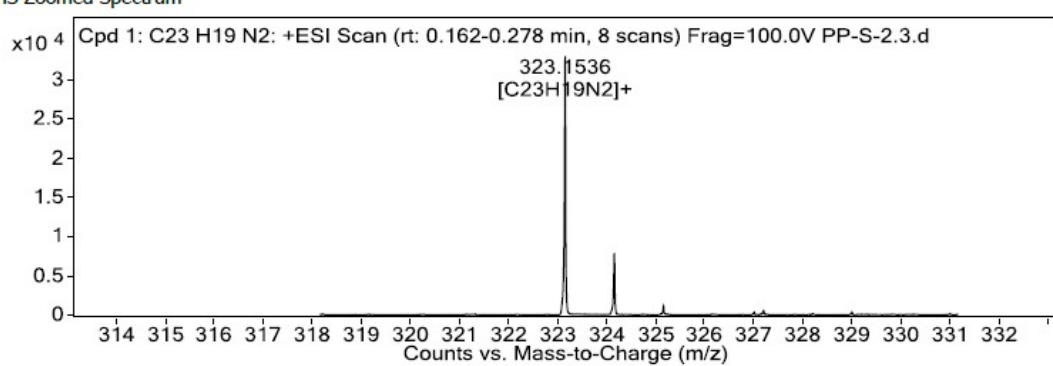


Fig. S6 HRMS of BPPyz

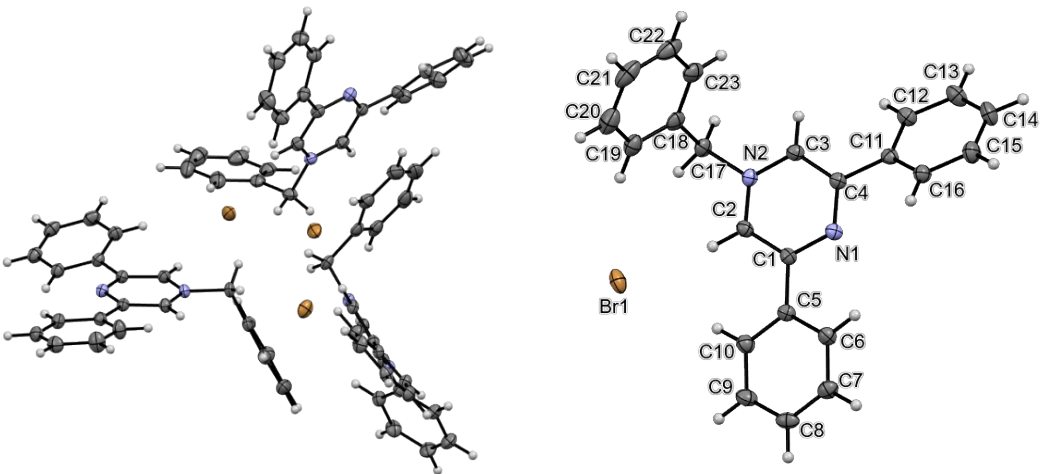


Fig. S7 ORTEP diagram of **BPPyz** three molecules appear in an asymmetric unit, for clarity only labelling is displayed for one of the three molecules. The thermal ellipsoids are drawn at the 50% probability level (CCDC 2189176)

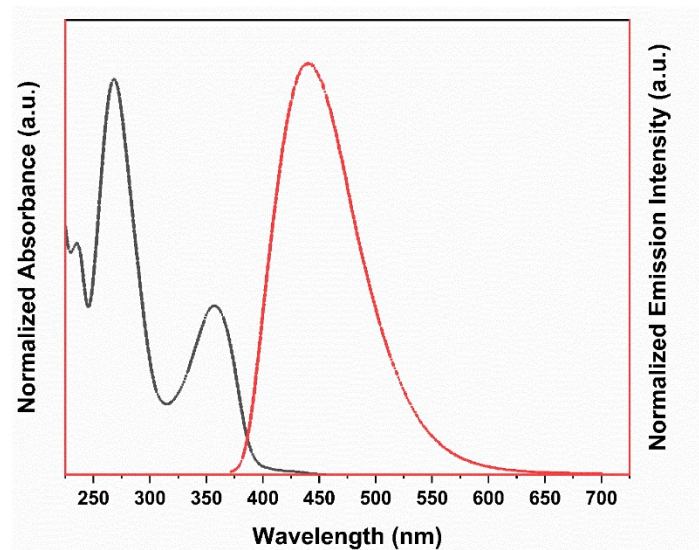


Fig. S8 UV-visible and fluorescence spectra of **BPPyz** ( $2 \times 10^{-5}$  M)

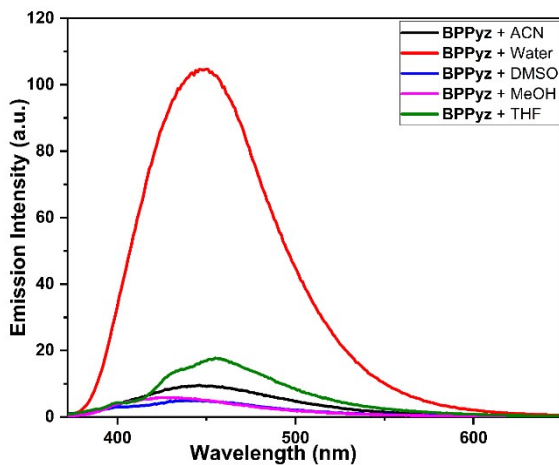


Fig. S9 Solvent study of **BPPyz** ( $2 \times 10^{-5}$  M)

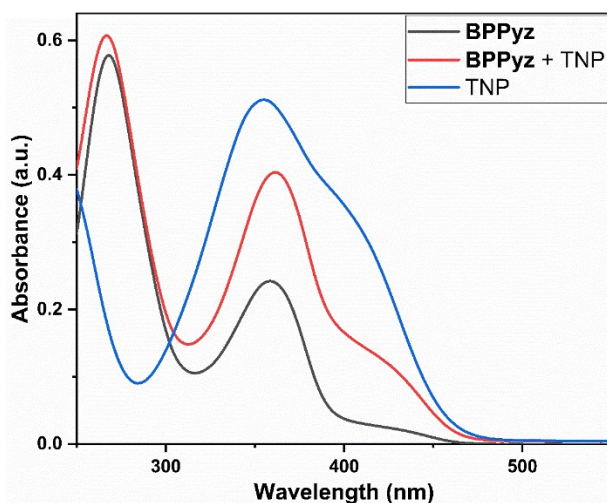


Fig. S10 Individual UV-visible spectra of **BPPyz**, **BPPyz-TNP** and **TNP**

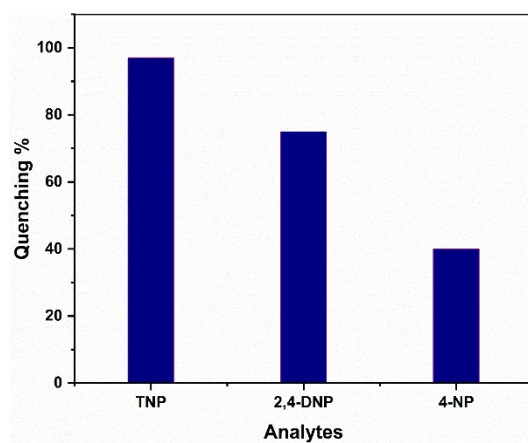


Fig. S11 Comparison of percentage fluorescence quenching obtained on addition of TNP, 2,4-DNP and 4-NP to the solution of **BPPyz** in water ( $2 \times 10^{-5}$  M)

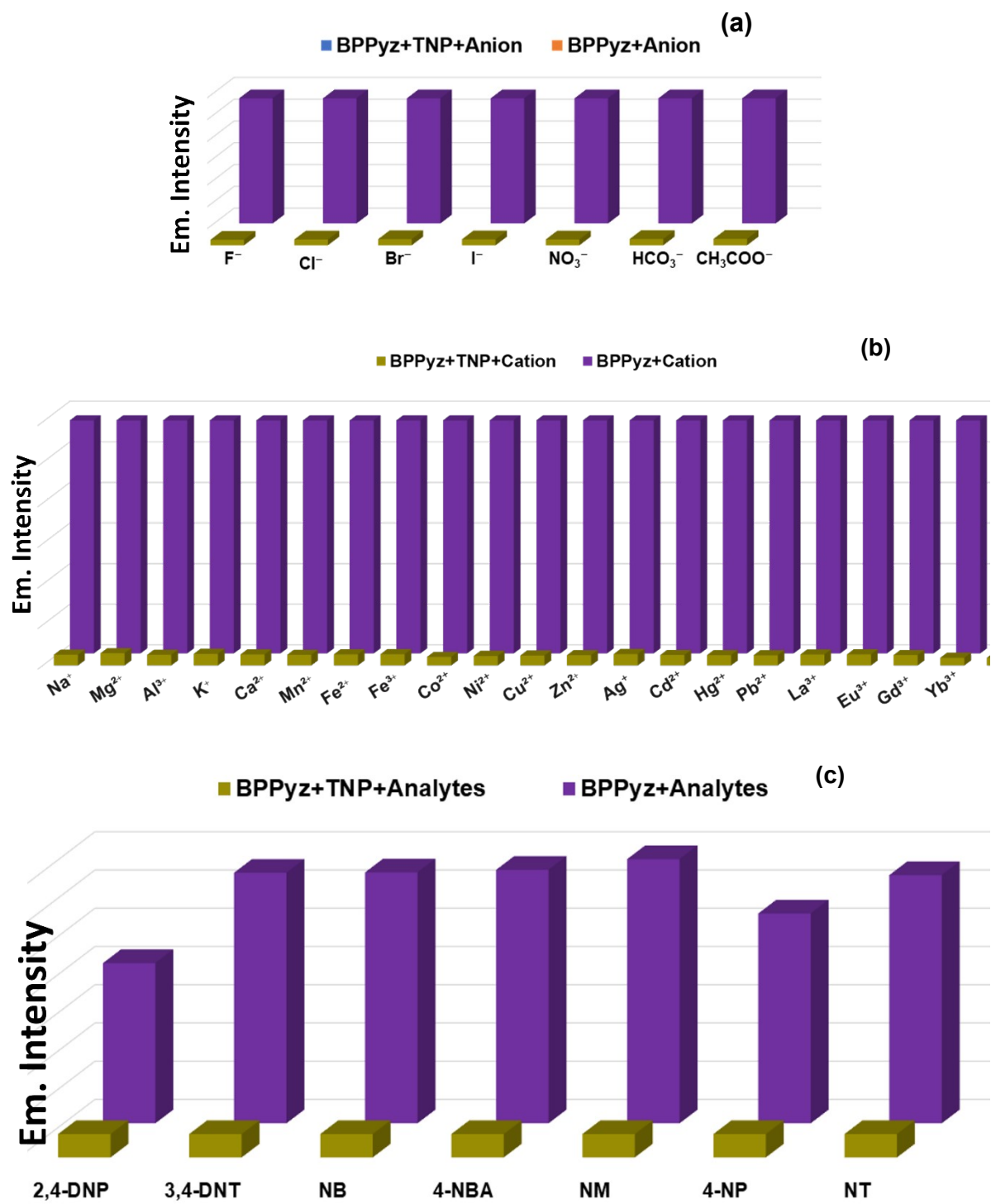


Fig. S12 Interference study of **BPPyz** toward TNP selectivity in the presence of (a) anions, (b) cations, and (c) organic analytes ( $2 \times 10^{-5}$  M)

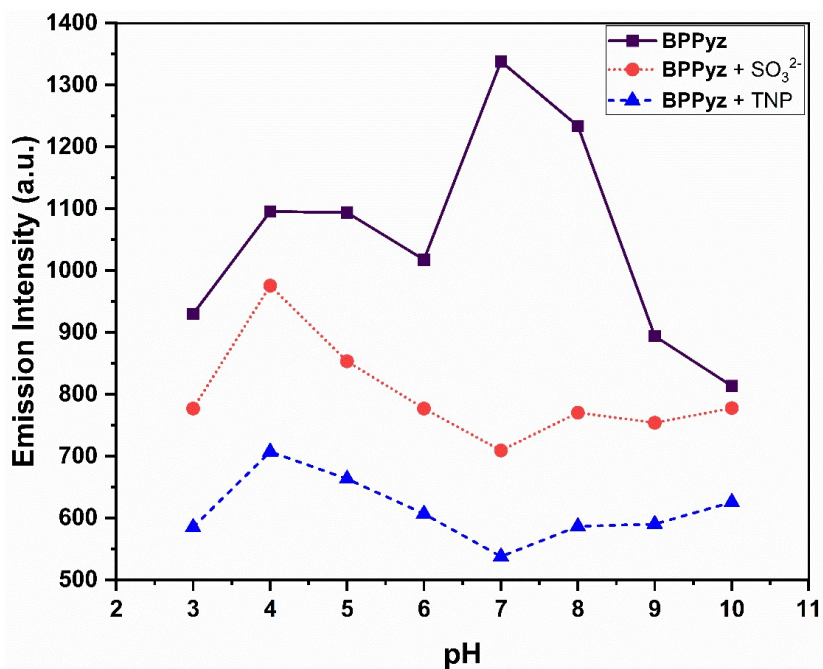


Fig. S13 Effect of pH on BPPyz, BPPyz + TNP and  $\text{BPPyz} + \text{SO}_3^{2-}$

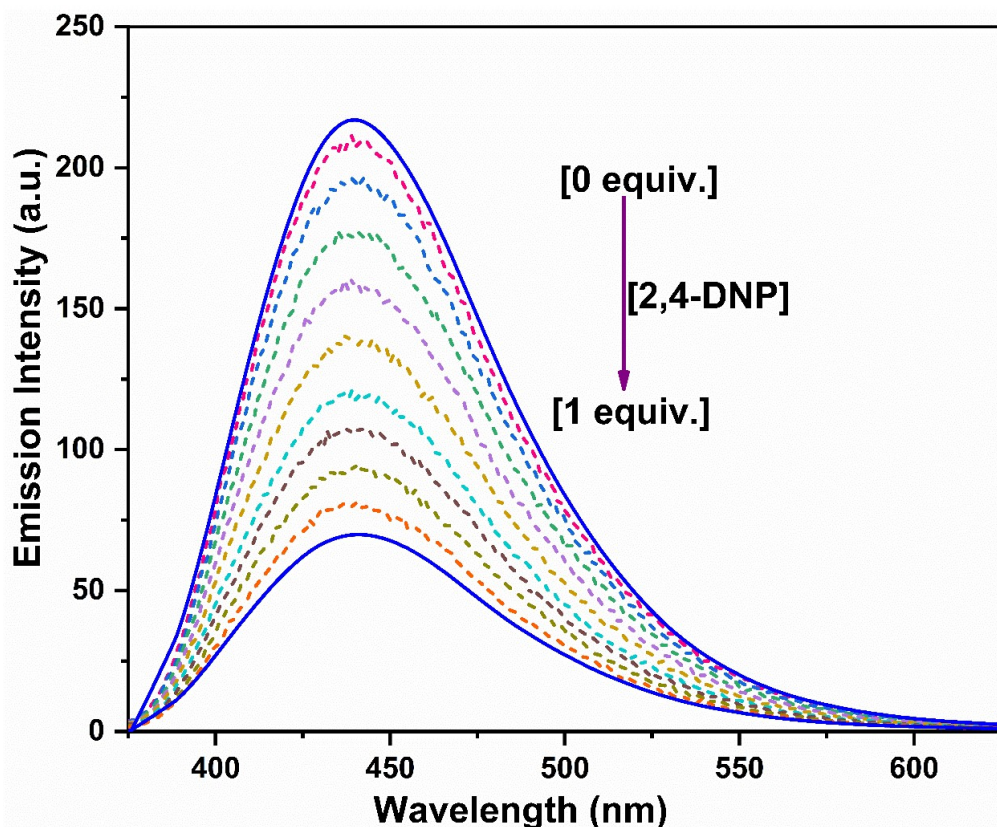


Fig. S14 Fluorescence spectra for BPPyz ( $2 \times 10^{-5}$  M) with different amounts of 2,4-DNP

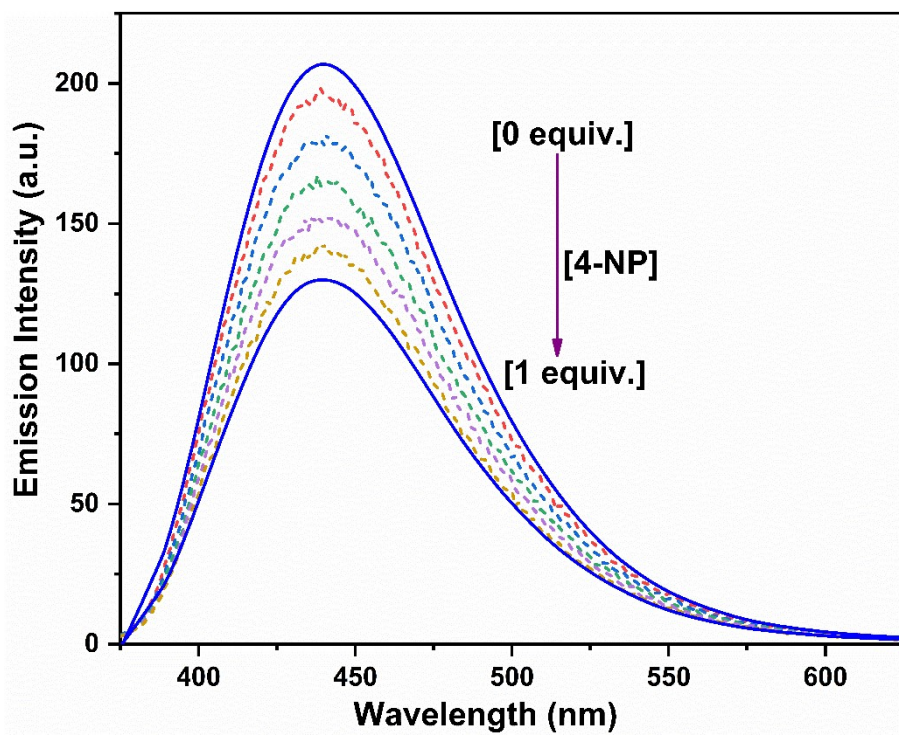


Fig. S15 Fluorescence spectra for BPPyz ( $2 \times 10^{-5}$  M) with different amounts of 4-NP

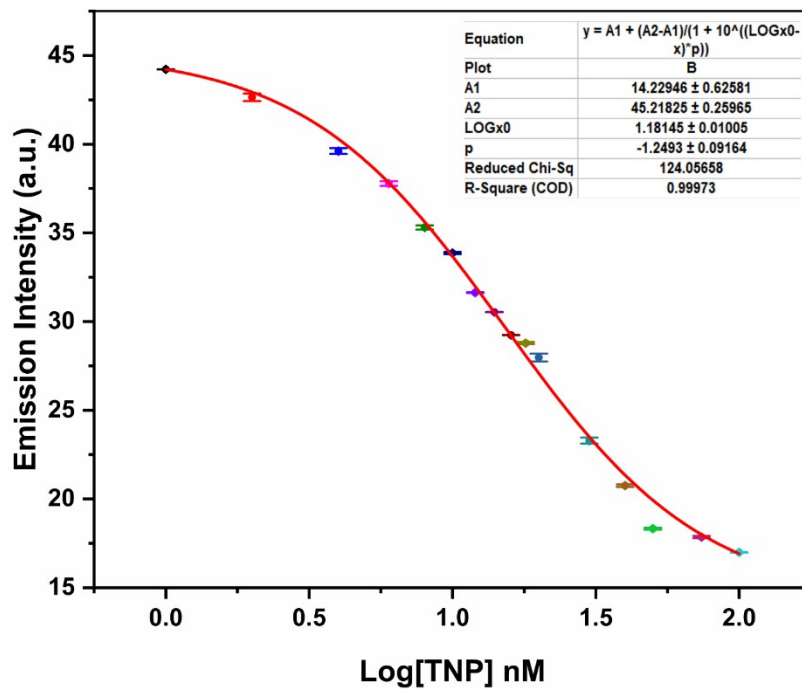


Fig. S16 Calibration curve with error bar for calculating Detection Limit of TNP

## Methods

### Photophysical studies

For photophysical studies, 10 mM stock solutions of **BPPyz** and different analytes (cations, anions and organic analytes) were prepared in Milli-Q water. The stock solutions of 4-nitrotoluene (NT), 3,4-dinitrotoluene (3,4-DNT), and 4-nitrobenzoic acid (NBA) were prepared in UV grade THF.

### Quantum yield calculation<sup>1</sup>

The fluorescence quantum yield was calculated using quinine sulfate as a reference in 0.1 M H<sub>2</sub>SO<sub>4</sub> ( $\Phi_R = 0.54$ ) and calculated using the following equation

$$\Phi_S = \Phi_R \frac{I_S}{I_R} \times \frac{A_R}{A_S} \times \frac{\eta_S^2}{\eta_R^2}$$

Where I = integrated area under the fluorescence curve, A = absorbance at the excitation wavelength,  $\eta$  = refractive index of the medium and  $\Phi$  = fluorescence quantum yield. Subscripts S and R refer to the sample and the reference standard, respectively.

### Fluorescence quenching percentage calculation<sup>2</sup>

The fluorescence quenching percentage was calculated using the equation.

$$\text{Fluorescence quenching \%} = \left(1 - \frac{I}{I_0}\right) \times 100\%$$

Where, I<sub>0</sub> = initial fluorescence intensity in the absence of analyte, I = fluorescence intensity in the presence of analyte.

### Overlap Integral Calculations<sup>3</sup>

Analytes Overlap integral values were calculated using the equation

$$J(\lambda) = F_D(\lambda) \varepsilon_A(\lambda) \lambda^4 d\lambda$$

Where  $F_D(\lambda)$  represents the corrected fluorescence intensity of donor in the range of  $\lambda$  to  $\lambda + \Delta\lambda$  with the total intensity normalized to unity.  $\varepsilon_A$  is the molar absorptivity of the acceptor at  $\lambda$  in M<sup>-1</sup> cm<sup>-1</sup>.

The Förster distance R<sub>0</sub> was calculated for **BPPyz**-TNP interaction using the equation

$$R_0 = 0.211 [(J)Q (\eta^{-4})(\kappa^2)]^{1/6}$$

Where J is the degree of spectral overlap between the donor fluorescence spectrum and the acceptor absorption spectrum. Q = 0.30; fluorescence quantum yield of the donor (without acceptor).  $\eta$  is the refractive index of the medium,  $\kappa^2$  (dipole orientation factor) = 0.667.

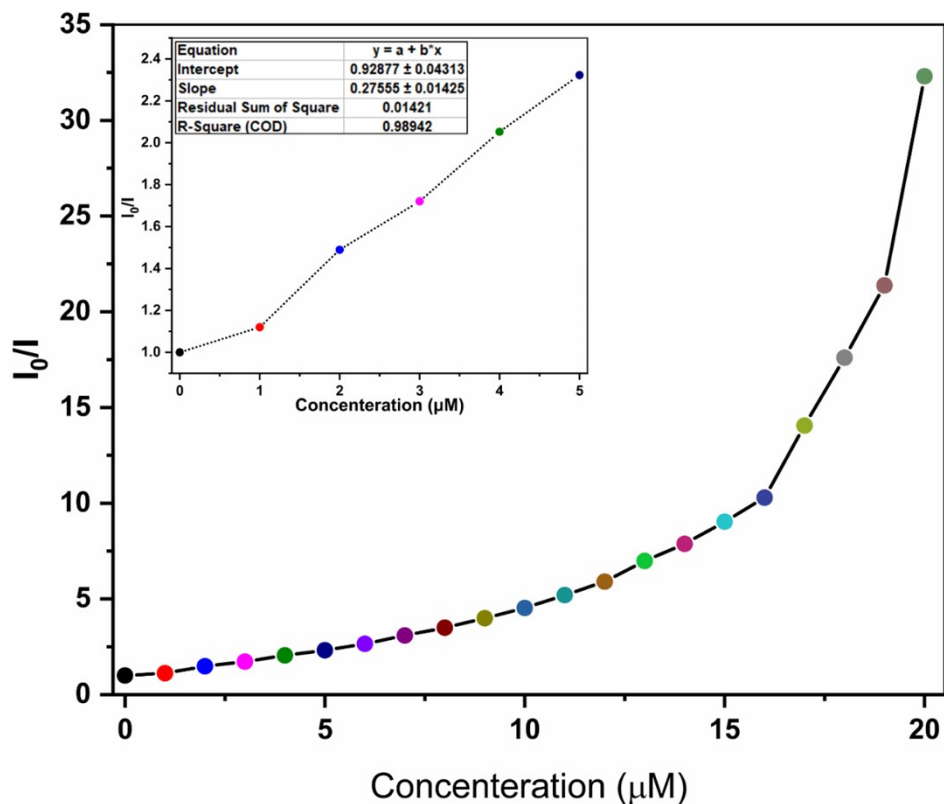


Fig. S17 Stern-Volmer plot of BPPyz using TNP as a quencher ( $2 \times 10^{-5} \text{ M}$ )

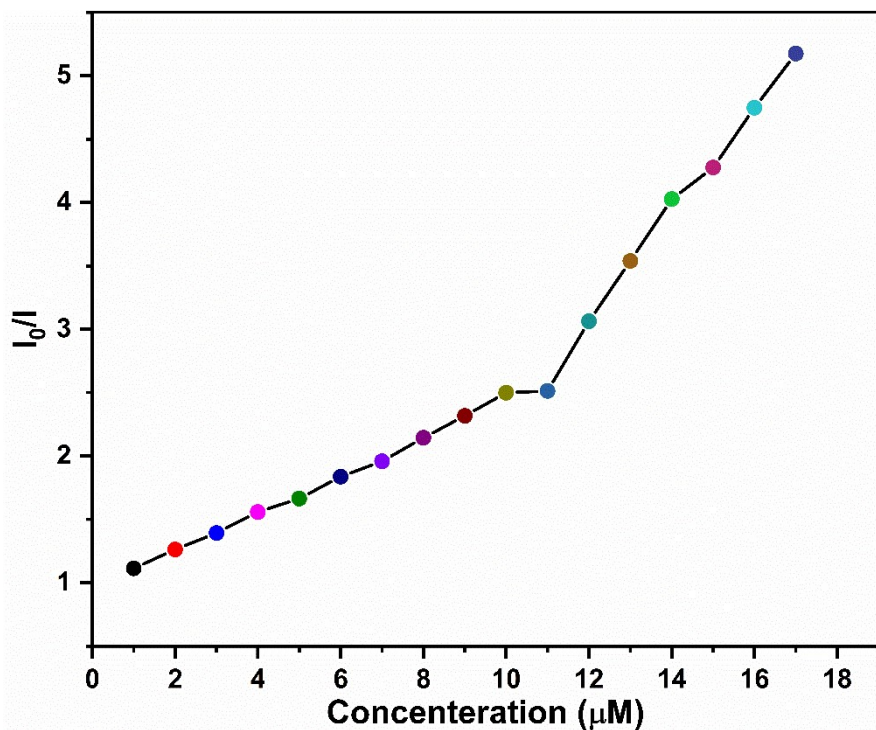


Fig. S18 Stern-Volmer plot of BPPyz using 2,4-DNP as a quencher ( $2 \times 10^{-5} \text{ M}$ )

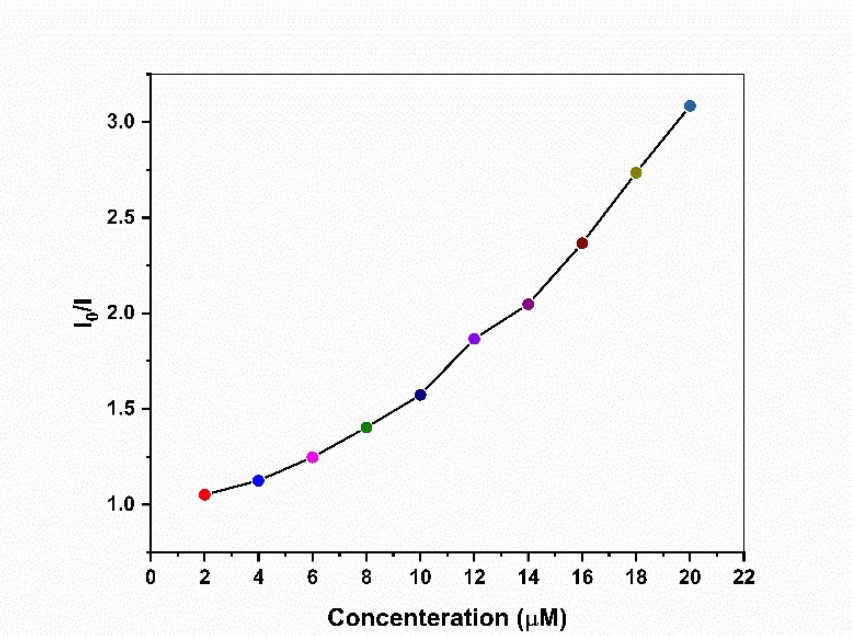


Fig. S19 Stern-Volmer plot of BPPyz using 4-NP as a quencher ( $2 \times 10^{-5}$  M)

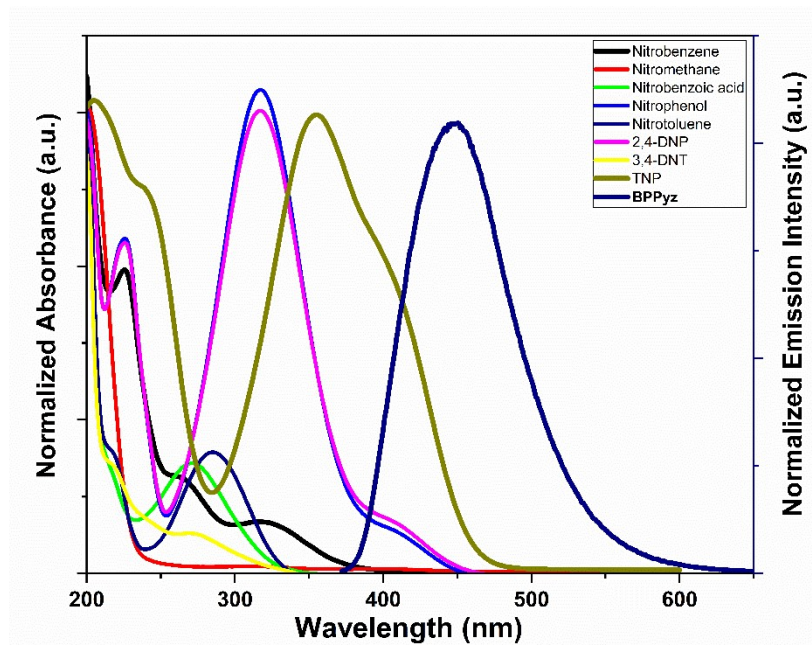


Fig. S20 Spectral overlap of organic analytes and BPPyz ( $2 \times 10^{-5}$  M)

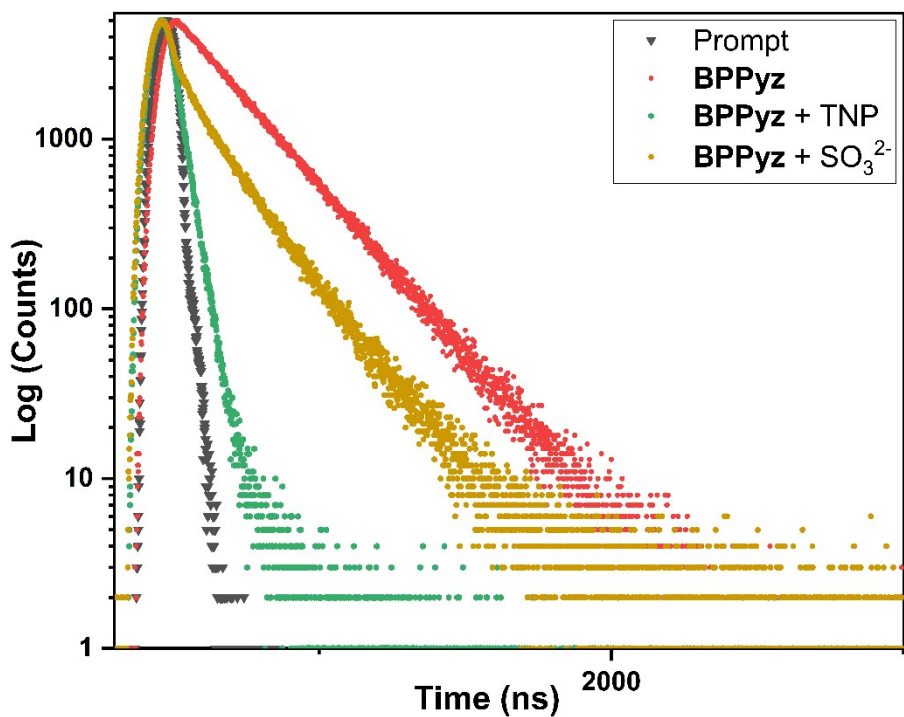


Fig. S21 Lifetime decay Plot of **BPPyz**, **BPPyz-TNP** and **BPPyz-SO<sub>3</sub><sup>2-</sup>** complexes ( $2 \times 10^{-5}$  M)

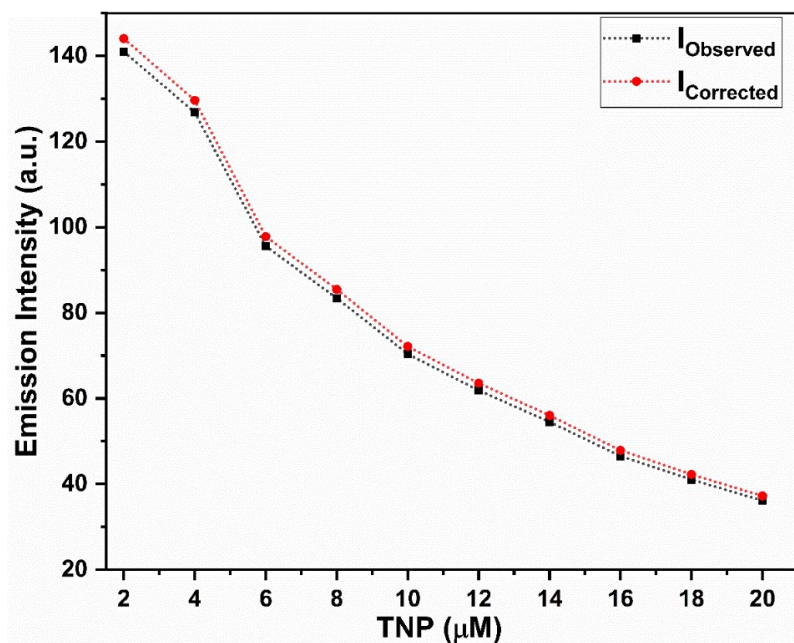


Fig. S22 Inner filter effect correction of **BPPyz** ( $2 \times 10^{-5}$  M)

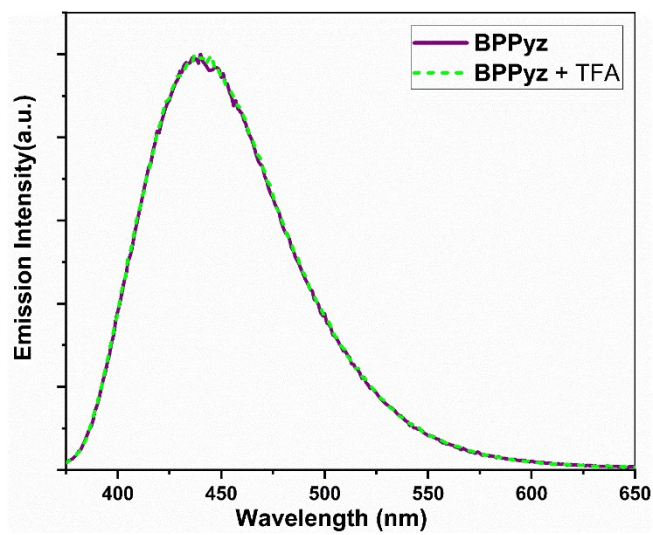


Fig. S23 Fluorescence spectra of **BPPyz** and **BPPyz** with TFA in aqueous medium ( $2 \times 10^{-5}$  M)

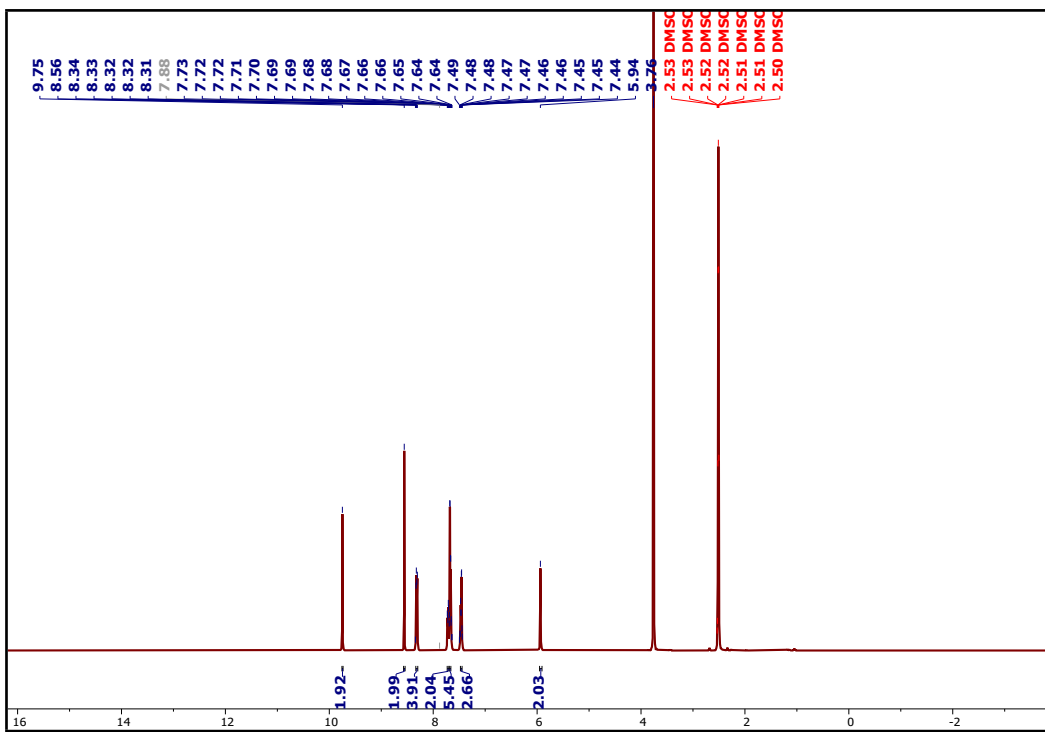


Fig. S24  $^1\text{H}$  NMR of **BPPyz**-TNP complex in  $\text{DMSO}-d_6$

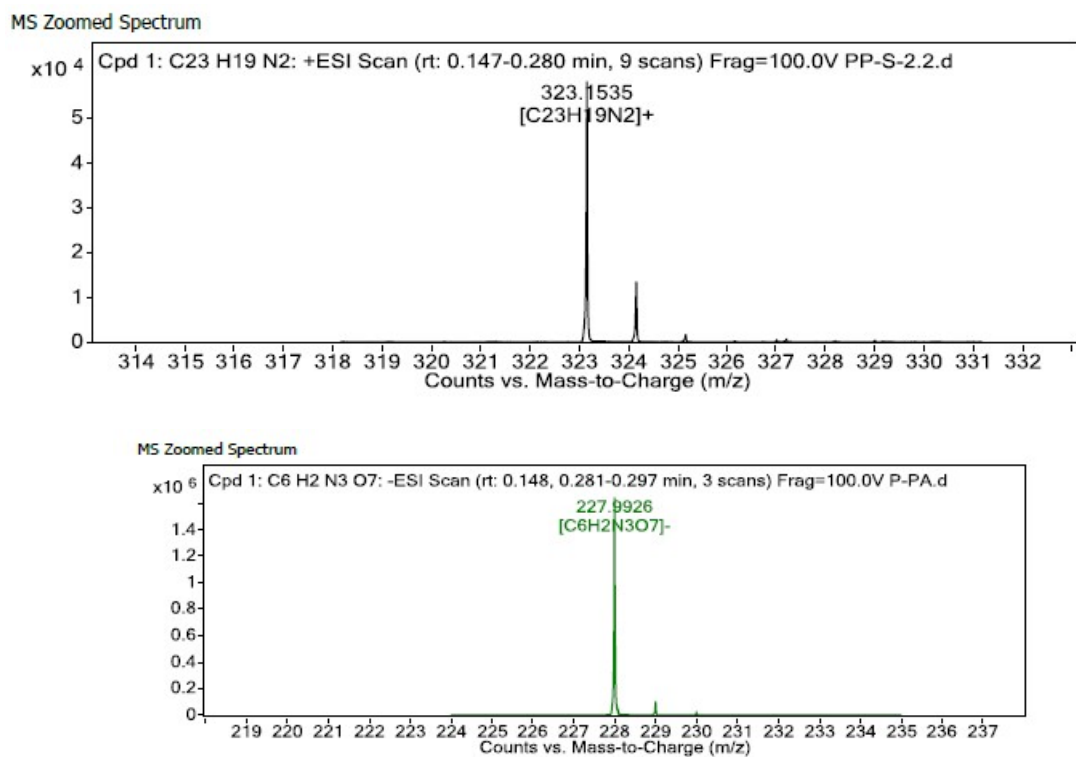


Fig. S25 HRMS of **BPPyz**-TNP complex

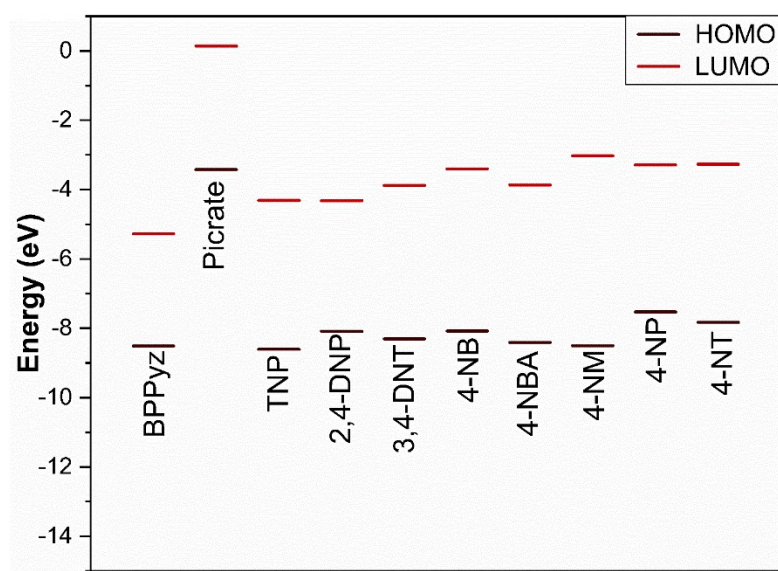


Fig. S26 HOMO-LUMO energy levels of **BPPyz** and organic analytes

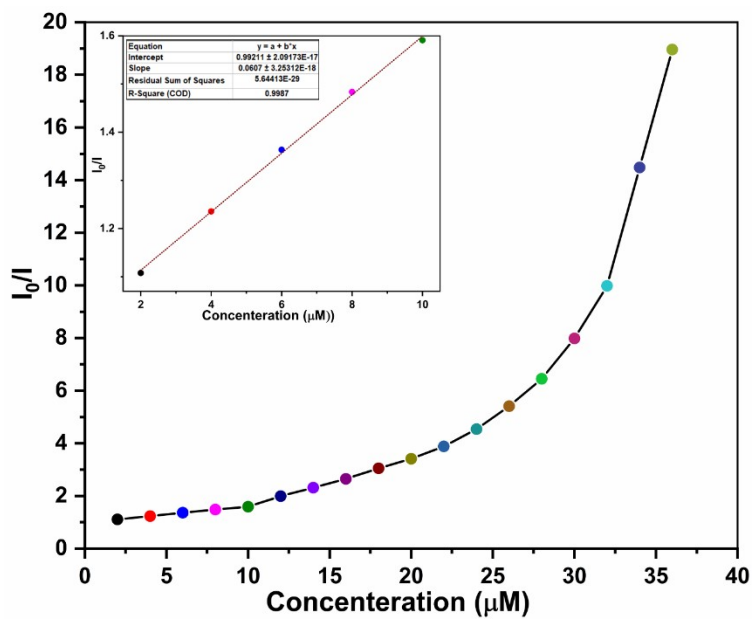


Fig. S27 Stern–Volmer plot of BPPyz using  $\text{SO}_3^{2-}$  as a quencher ( $2 \times 10^{-5} \text{ M}$ )

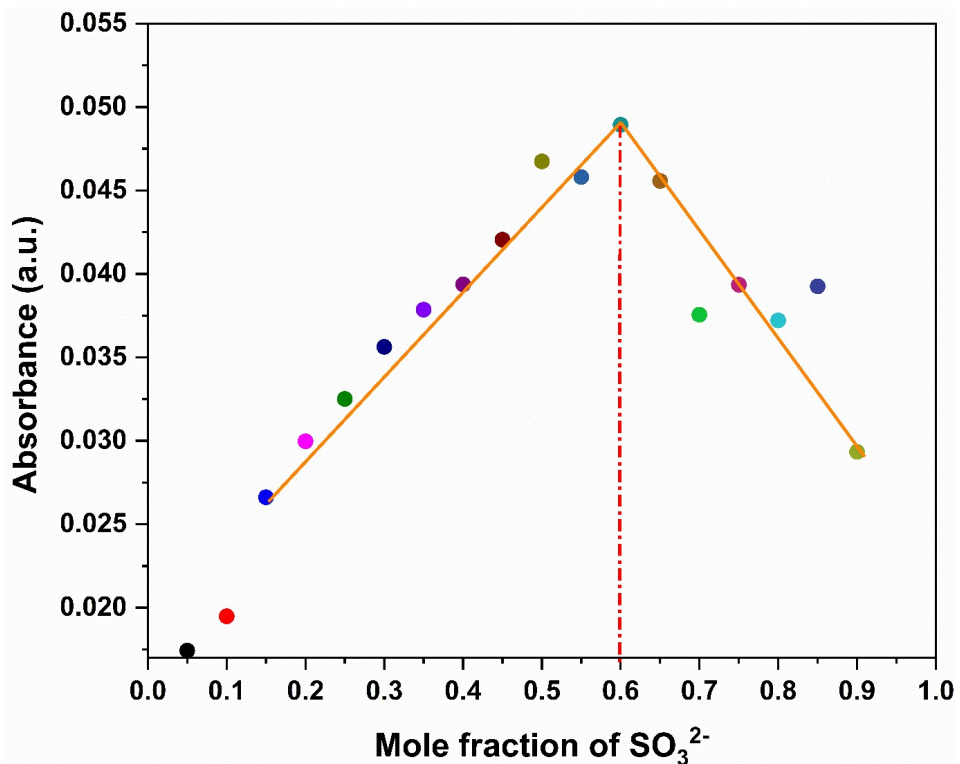


Fig. S28 Job's Plot of BPPyz with  $\text{SO}_3^{2-}$  ( $2 \times 10^{-5} \text{ M}$ )

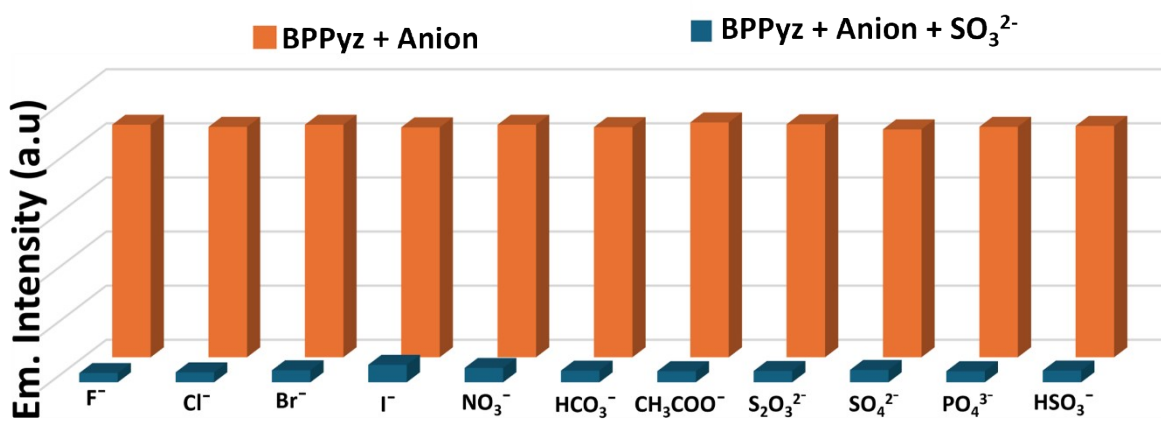


Fig. S29 Selectivity of BPPyz toward SO<sub>3</sub><sup>2-</sup> in the presence of anions ( $2 \times 10^{-5}$  M)

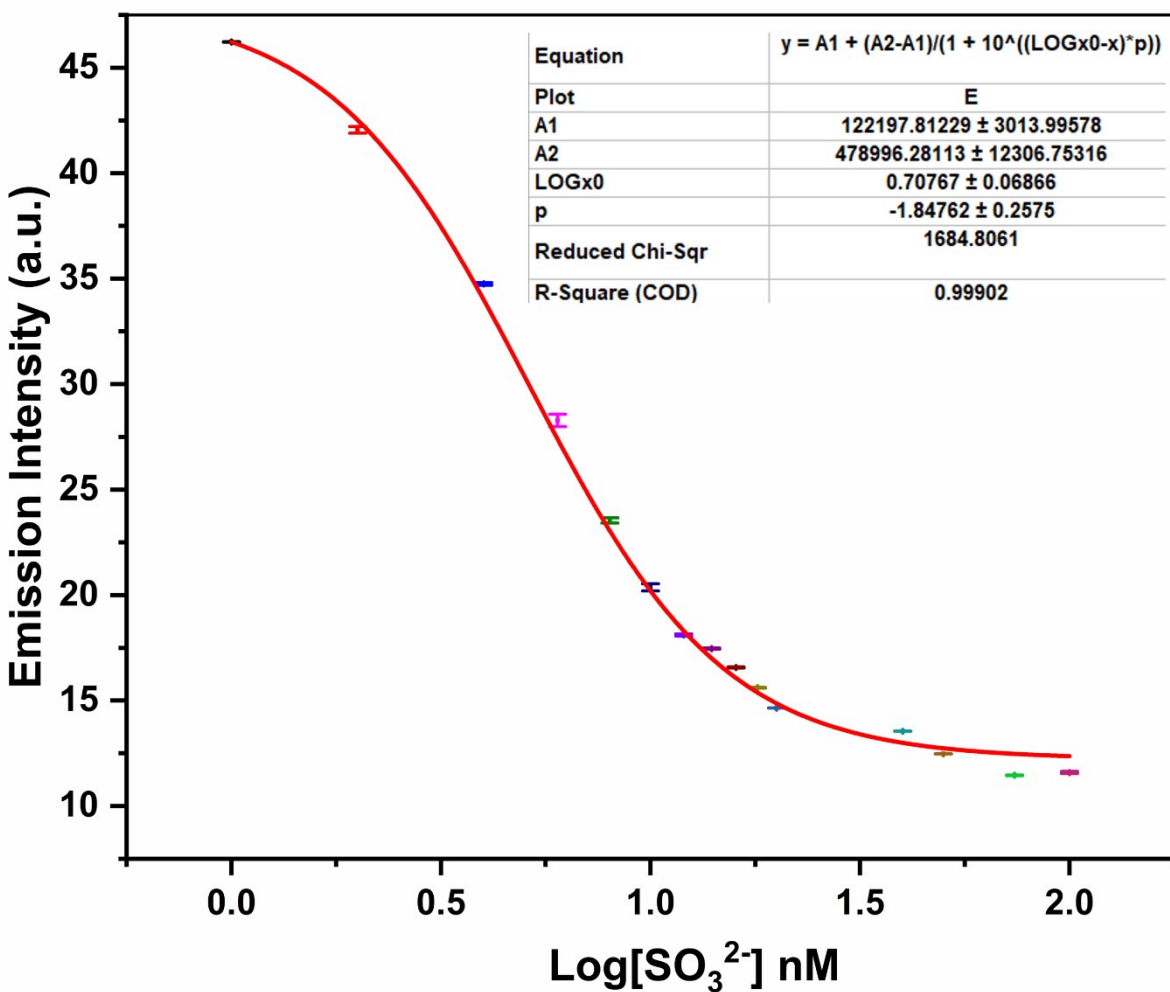


Fig. S30 Calibration curve with error bar for calculating Detection Limit of SO<sub>3</sub><sup>2-</sup>

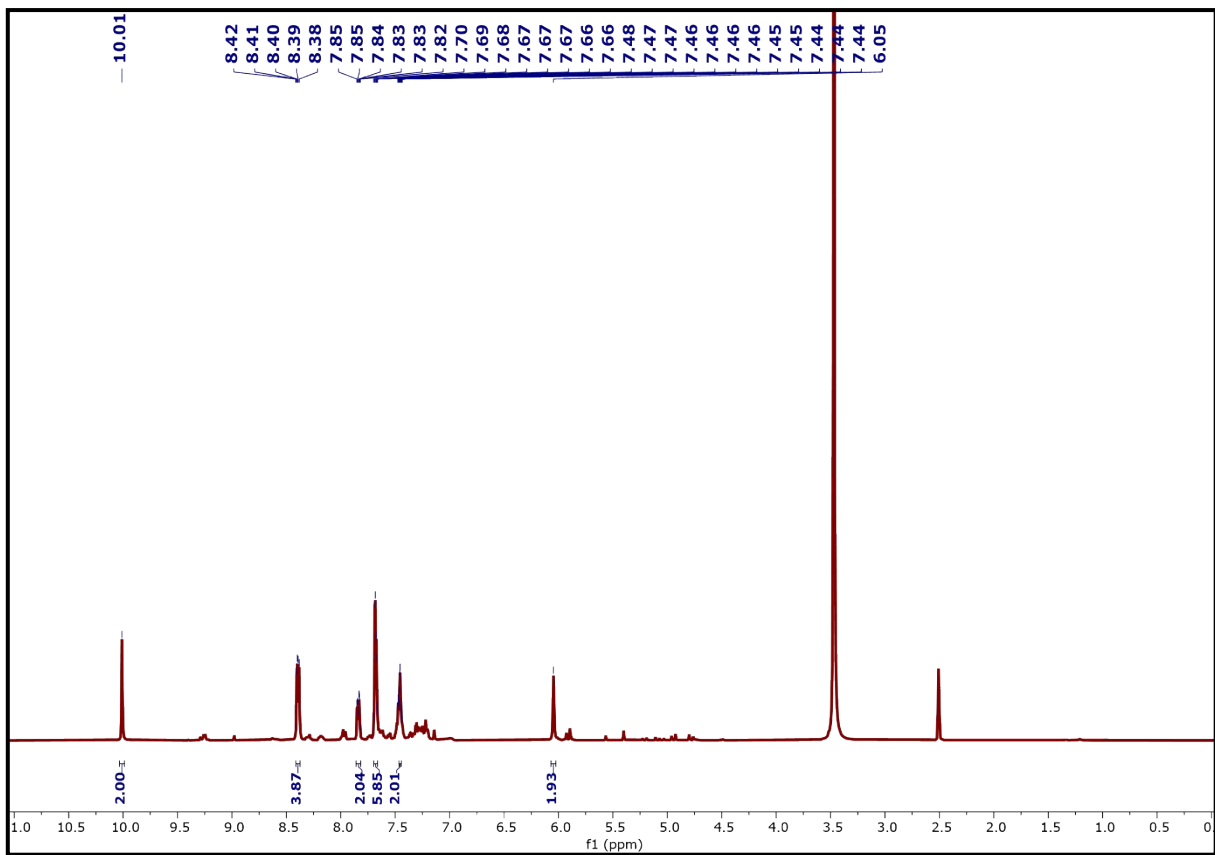


Fig. S31  $^1\text{H}$  NMR of  $\text{BPPyz-SO}_3^{2-}$  complex in  $\text{DMSO}-d_6$

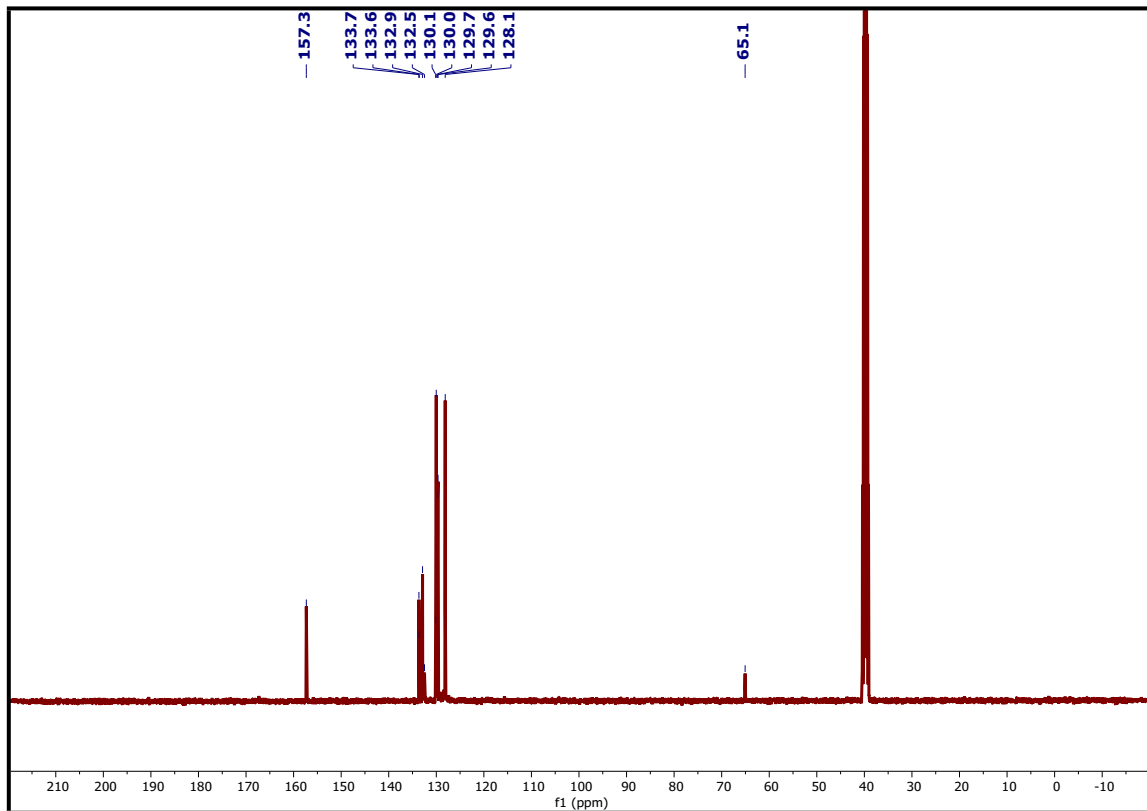


Fig. S32  $^{13}\text{C}$  NMR of  $\text{BPPyz-SO}_3^{2-}$  complex in  $\text{DMSO}-d_6$

MS Zoomed Spectrum

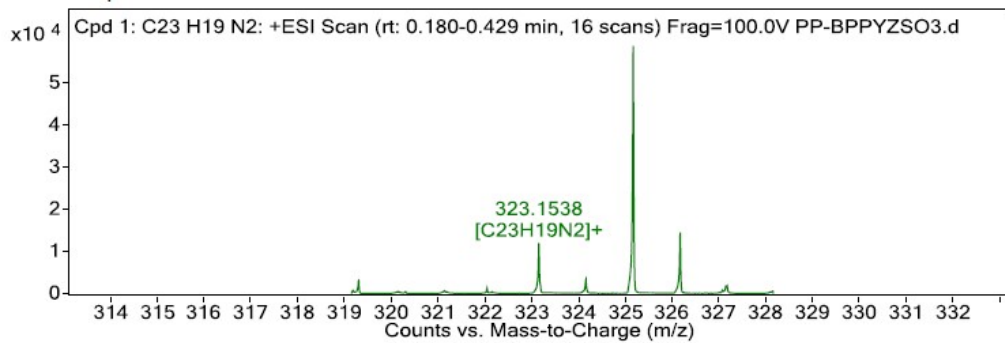
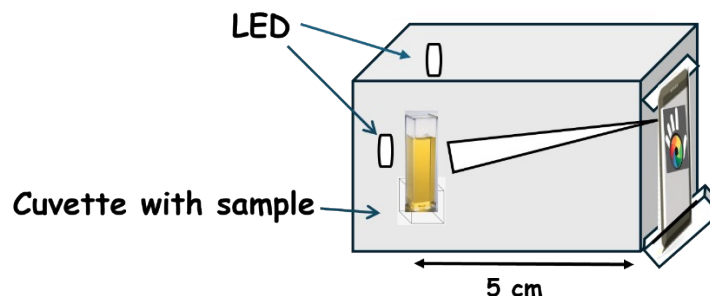
Fig. S33 HRMS of BPPyz-SO<sub>3</sub><sup>2-</sup> complex

Fig. S34 Sketch of Photo light box for RGB analysis

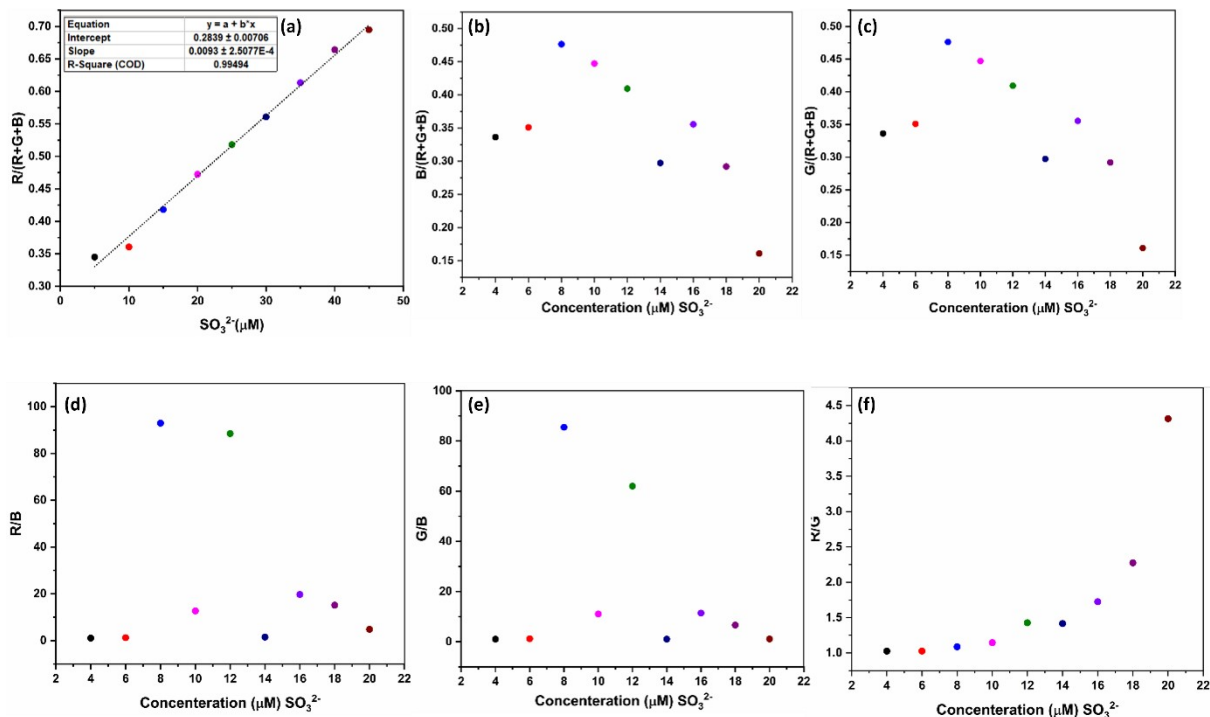
Fig. S35 The ratio of RGB (a) R/(R+G+B) (b) G/(R+G+B) (c) B/(R+G+B) (d) R/G (e) R/B (f) G/B versus SO<sub>3</sub><sup>2-</sup> concentration in the range of 0 to 20.0 μM

Table S1. Single-crystal XRD data and structure refinement of **BPPyz** and **BPPyz-TNP** complex

Identification code	<b>BPPyz</b>	<b>BPPyz-TNP</b>
Empirical formula	C <sub>23</sub> H <sub>19</sub> BrN <sub>2</sub>	C <sub>29</sub> H <sub>21</sub> N <sub>5</sub> O <sub>7</sub>
Formula weight	403.31	551.51
Temperature/K	93(2)	93(2)
Crystal system	monoclinic	monoclinic
Space group	P2 <sub>1</sub> /c	C2/c
a/Å	23.0173(3)	17.3755(2)
b/Å	10.11520(10)	19.6061(2)
c/Å	26.4430(3)	15.0107(2)
α/°	90	90
β/°	113.4840(10)	103.3710(10)
γ/°	90	90
Volume/Å <sup>3</sup>	5646.64(12)	4975.02(10)
Z	12	8
ρ <sub>calc</sub> g/cm <sup>3</sup>	1.423	1.473
μ/mm <sup>-1</sup>	3.023	0.903
F(000)	2472.0	2288.0
Crystal size/mm <sup>3</sup>	0.13 × 0.08 × 0.05	0.14 × 0.12 × 0.1
Radiation	Cu Kα (λ = 1.54184)	Cu Kα (λ = 1.54184)
2Θ range for data collection/°	8.376 to 159.512	6.904 to 159.878
Index ranges	-28 ≤ h ≤ 29, -12 ≤ k ≤ 6, -28 ≤ l ≤ 33	-11 ≤ h ≤ 21, -24 ≤ k ≤ 24, -18 ≤ l ≤ 19
Reflections collected	35513	15324
Independent reflections	12044 [R <sub>int</sub> = 0.0318, R <sub>sigma</sub> = 0.0322]	5281 [R <sub>int</sub> = 0.0248, R <sub>sigma</sub> = 0.0244]
Data/restraints/parameters	12044/0/703	5281/0/371
Goodness-of-fit on F <sup>2</sup>	1.076	1.058
Final R indexes [I>=2σ (I)]	R <sub>1</sub> = 0.0361, wR <sub>2</sub> = 0.0999	R <sub>1</sub> = 0.0557, wR <sub>2</sub> = 0.1389
Final R indexes [all data]	R <sub>1</sub> = 0.0383, wR <sub>2</sub> = 0.1014	R <sub>1</sub> = 0.0592, wR <sub>2</sub> = 0.1412
Largest diff.peak/hole / e Å <sup>-3</sup>	0.72/-0.71	0.70/-0.72
CCDC	2189176	2189177

Table S2. Bond Lengths for **BPPyz**

<b>Atom</b>	<b>Atom</b>	<b>Length/Å</b>	<b>Atom</b>	<b>Atom</b>	<b>Length/Å</b>
N1	C4	1.338(3)	C8	C9	1.385(3)
N1	C1	1.343(2)	C7	C6	1.381(3)
N201	C201	1.336(3)	C219	C220	1.394(3)
N201	C204	1.336(3)	C311	C316	1.400(3)
N202	C203	1.338(3)	C311	C312	1.396(3)
N202	C202	1.341(3)	C211	C216	1.397(3)
N202	C217	1.501(2)	C211	C212	1.398(3)
N2	C3	1.345(3)	C18	C23	1.397(3)
N2	C2	1.343(3)	C18	C19	1.397(3)
N2	C17	1.503(2)	C223	C222	1.387(3)
N302	C302	1.341(3)	C208	C207	1.381(3)
N302	C303	1.340(3)	C208	C209	1.385(3)
N302	C317	1.500(3)	C216	C215	1.389(3)
N301	C304	1.341(3)	C305	C306	1.398(3)
N301	C301	1.345(3)	C305	C310	1.395(3)
C4	C3	1.397(3)	C23	C22	1.391(3)
C4	C11	1.476(3)	C306	C307	1.386(3)
C11	C12	1.397(3)	C13	C14	1.387(3)
C11	C16	1.401(3)	C222	C221	1.397(3)
C5	C1	1.475(3)	C221	C220	1.378(4)
C5	C10	1.393(3)	C15	C14	1.391(3)
C5	C6	1.399(3)	C318	C323	1.397(3)
C2	C1	1.396(3)	C318	C317	1.508(3)
C201	C205	1.484(3)	C318	C319	1.392(3)
C201	C202	1.404(3)	C212	C213	1.392(3)
C218	C217	1.513(3)	C210	C209	1.389(3)
C218	C219	1.388(3)	C307	C308	1.387(3)
C218	C223	1.394(3)	C215	C214	1.389(3)
C204	C203	1.399(3)	C323	C322	1.387(3)
C204	C211	1.475(3)	C316	C315	1.393(3)
C206	C205	1.402(3)	C214	C213	1.378(3)
C206	C207	1.387(3)	C313	C312	1.391(3)
C304	C311	1.480(3)	C313	C314	1.379(4)
C304	C303	1.395(3)	C22	C21	1.384(4)
C12	C13	1.390(3)	C308	C309	1.382(4)
C16	C15	1.389(3)	C19	C20	1.392(3)
C17	C18	1.507(3)	C314	C315	1.392(3)
C10	C9	1.388(3)	C310	C309	1.388(3)
C205	C210	1.393(3)	C319	C320	1.395(4)
C301	C302	1.398(3)	C322	C321	1.391(4)
C301	C305	1.475(3)	C20	C21	1.380(4)
C8	C7	1.387(3)	C320	C321	1.386(5)

Table S3. Bond Angles for **BPPyz**

<b>Atom</b>	<b>Atom</b>	<b>Atom</b>	<b>Angle/°</b>	<b>Atom</b>	<b>Atom</b>	<b>Atom</b>	<b>Angle/°</b>
C4	N1	C1	118.96(17)	C316	C311	C304	120.07(19)
C201	N201	C204	119.31(17)	C312	C311	C304	120.66(19)
C203	N202	C202	121.49(17)	C312	C311	C316	119.27(19)
C203	N202	C217	118.69(17)	C7	C6	C5	120.35(19)
C202	N202	C217	119.79(17)	C216	C211	C204	118.78(18)
C3	N2	C17	119.51(16)	C212	C211	C204	121.37(19)
C2	N2	C3	121.09(17)	C212	C211	C216	119.84(19)
C2	N2	C17	119.40(16)	C23	C18	C17	120.2(2)
C302	N302	C317	119.61(17)	C23	C18	C19	119.8(2)
C303	N302	C302	121.10(18)	C19	C18	C17	120.0(2)
C303	N302	C317	119.29(17)	C8	C9	C10	120.7(2)
C304	N301	C301	118.59(18)	C222	C223	C218	120.2(2)
N1	C4	C3	121.30(18)	N302	C303	C304	119.10(19)
N1	C4	C11	116.95(17)	C207	C208	C209	119.6(2)
C3	C4	C11	121.74(17)	C215	C216	C211	119.7(2)
N2	C3	C4	118.67(18)	C306	C305	C301	119.40(19)
C12	C11	C4	120.75(18)	C310	C305	C301	121.06(19)
C12	C11	C16	119.66(19)	C310	C305	C306	119.5(2)
C16	C11	C4	119.57(18)	C22	C23	C18	120.0(2)
C10	C5	C1	121.51(18)	C307	C306	C305	120.2(2)
C10	C5	C6	119.28(18)	C14	C13	C12	120.4(2)
C6	C5	C1	119.18(17)	C223	C222	C221	119.7(2)
N2	C2	C1	118.96(17)	C220	C221	C222	120.1(2)
N1	C1	C5	117.08(17)	C16	C15	C14	119.8(2)
N1	C1	C2	121.00(18)	C323	C318	C317	120.1(2)
C2	C1	C5	121.91(17)	C319	C318	C323	119.8(2)
N201	C201	C205	117.81(17)	C319	C318	C317	120.1(2)
N201	C201	C202	120.88(18)	C221	C220	C219	120.2(2)
C202	C201	C205	121.31(18)	C208	C207	C206	120.5(2)
C219	C218	C217	119.62(19)	C213	C212	C211	119.6(2)
C219	C218	C223	119.8(2)	C209	C210	C205	120.0(2)
C223	C218	C217	120.45(19)	C306	C307	C308	119.9(2)
N201	C204	C203	121.06(18)	C216	C215	C214	120.3(2)
N201	C204	C211	118.23(17)	C322	C323	C318	120.5(2)
C203	C204	C211	120.68(18)	N302	C317	C318	110.49(16)
C207	C206	C205	120.1(2)	C315	C316	C311	120.2(2)
N202	C203	C204	118.67(18)	C213	C214	C215	120.1(2)
N301	C304	C311	118.98(18)	C314	C313	C312	120.6(2)
N301	C304	C303	121.18(19)	C208	C209	C210	120.7(2)
C303	C304	C311	119.80(18)	C313	C312	C311	120.0(2)
C13	C12	C11	119.7(2)	C13	C14	C15	120.2(2)
C15	C16	C11	120.2(2)	C21	C22	C23	120.0(2)

N2	C17	C18	110.21(16)	C309	C308	C307	120.2(2)
C9	C10	C5	119.8(2)	C214	C213	C212	120.4(2)
C206	C205	C201	119.21(18)	C20	C19	C18	119.4(2)
C210	C205	C201	121.68(18)	C313	C314	C315	120.0(2)
C210	C205	C206	119.10(19)	C314	C315	C316	119.9(2)
N202	C202	C201	118.58(18)	C309	C310	C305	119.8(2)
N202	C217	C218	112.06(16)	C308	C309	C310	120.4(2)
N301	C301	C302	121.28(18)	C318	C319	C320	119.6(3)
N301	C301	C305	118.83(18)	C323	C322	C321	119.5(3)
C302	C301	C305	119.88(19)	C21	C20	C19	120.6(3)
N302	C302	C301	118.74(19)	C20	C21	C22	120.3(2)
C9	C8	C7	119.6(2)	C321	C320	C319	120.1(3)
C6	C7	C8	120.3(2)	C320	C321	C322	120.5(3)
C218	C219	C220	119.9(2)				

Table S4. Bond Lengths for BPPyz-TNP complex

Atom	Atom	Length/Å	Atom	Atom	Length/Å
O1	C24	1.239(2)	C7	C8	1.389(3)
O2	N3	1.185(3)	C8	C9	1.384(3)
O3	N3	1.206(3)	C9	C10	1.387(3)
O4	N4	1.231(3)	C11	C12	1.396(3)
O5	N4	1.237(3)	C11	C16	1.401(3)
O6	N5	1.234(2)	C12	C13	1.385(3)
O7	N5	1.222(2)	C13	C14	1.388(3)
N1	C1	1.341(2)	C14	C15	1.386(3)
N1	C4	1.340(2)	C15	C16	1.385(3)
N2	C2	1.343(2)	C17	C18	1.506(3)
N2	C3	1.338(2)	C18	C19	1.382(3)
N2	C17	1.502(2)	C18	C23	1.391(3)
N3	C25	1.455(3)	C19	C20	1.393(3)
N4	C27	1.439(3)	C20	C21	1.369(4)
N5	C29	1.453(2)	C21	C22	1.385(3)
C1	C2	1.396(2)	C22	C23	1.387(3)
C1	C5	1.479(2)	C24	C25	1.464(2)
C3	C4	1.401(2)	C24	C29	1.457(2)
C4	C11	1.477(2)	C25	C26	1.373(3)
C5	C6	1.397(3)	C26	C27	1.378(3)
C5	C10	1.397(3)	C27	C28	1.392(3)
C6	C7	1.384(3)	C28	C29	1.365(3)

Table S5. Bond Angles for **BPPyz**-TNP complex

<b>Atom</b>	<b>Atom</b>	<b>Atom</b>	<b>Angle/°</b>	<b>Atom</b>	<b>Atom</b>	<b>Atom</b>	<b>Angle/°</b>
C4	N1	C1	119.95(15)	C12	C11	C16	118.95(17)
C2	N2	C17	119.01(15)	C16	C11	C4	119.86(17)
C3	N2	C2	121.75(15)	C13	C12	C11	120.47(18)
C3	N2	C17	119.21(16)	C12	C13	C14	120.26(19)
O2	N3	O3	121.6(2)	C15	C14	C13	119.68(19)
O2	N3	C25	120.0(2)	C16	C15	C14	120.51(19)
O3	N3	C25	118.3(2)	C15	C16	C11	120.12(19)
O4	N4	O5	123.3(2)	N2	C17	C18	110.26(15)
O4	N4	C27	119.1(2)	C19	C18	C17	120.76(19)
O5	N4	C27	117.5(2)	C19	C18	C23	119.30(19)
O6	N5	C29	117.68(17)	C23	C18	C17	119.94(18)
O7	N5	O6	123.56(18)	C18	C19	C20	120.1(2)
O7	N5	C29	118.75(16)	C21	C20	C19	120.5(2)
N1	C1	C2	120.34(17)	C20	C21	C22	119.8(2)
N1	C1	C5	117.69(15)	C21	C22	C23	120.1(2)
C2	C1	C5	121.96(16)	C22	C23	C18	120.1(2)
N2	C2	C1	118.83(16)	O1	C24	C25	125.18(17)
N2	C3	C4	118.54(17)	O1	C24	C29	123.70(16)
N1	C4	C3	120.57(16)	C29	C24	C25	111.00(15)
N1	C4	C11	117.81(15)	N3	C25	C24	119.47(17)
C3	C4	C11	121.62(16)	C26	C25	N3	116.37(18)
C6	C5	C1	119.23(17)	C26	C25	C24	124.16(18)
C10	C5	C1	121.85(16)	C25	C26	C27	119.47(18)
C10	C5	C6	118.92(17)	C26	C27	N4	119.3(2)
C7	C6	C5	120.37(18)	C26	C27	C28	121.22(18)
C6	C7	C8	120.18(19)	C28	C27	N4	119.5(2)
C9	C8	C7	119.97(19)	C29	C28	C27	119.01(18)
C8	C9	C10	120.07(19)	N5	C29	C24	118.61(15)
C9	C10	C5	120.46(18)	C28	C29	N5	116.60(16)

Table S6: A comparison of literature reported Chemosensors for TNP detection

S.No.	Publication	Material used	Detection Limit	Stern-Volmer constant
1	Present Study	Pyrazinium-based	9 nM	$4.12 \times 10^5 \text{ M}^{-1}$
2	<i>Ind. Eng. Chem. Res</i> , 2021, <b>60</b> , 7987–7997	Triazine-based	209 nM	1.02 mM
3	<i>ACS Appl. Mater. Interfaces</i> , 2015, <b>7</b> , 10491–10500	Benzimidazolium-based	$5 \times 10^{-13} \text{ M}$	$4.8 \times 10^5 \text{ M}^{-1}$
4	<i>Sens. Actuators B Chem.</i> , 2016, <b>231</b> , 293–301	Imidazolium-based	10 nM	$1.01 \times 10^6 \text{ M}^{-1}$
5	<i>Chemosphere</i> , 2022, <b>2</b> , 131825	Benzimidazolium-based	282 nM	$2.32 \times 10^6 \text{ M}^{-1}$
6	<i>ACS Appl. Mater. Interfaces</i> , 2016, <b>8</b> , 38, 25326–25336	Imidazolium-naphthalene diimide based	34.8 nM	$5.85 \times 10^4 \text{ M}^{-1}$
7	<i>New J. Chem</i> , 2022, <b>46</b> , 16907-16913	Pyrazinium-based	11.6 nM	$3.8 \times 10^4 \text{ M}^{-1}$

Table S7: A comparison of literature reported Chemosensors for  $\text{SO}_3^{2-}$  detection

S. No	Publication	Material used	Detection Limit	S-V constant	Medium used	Colorimetric/ Fluorometric
1	Present Study	Pyrazinium-based	31 nM	$3.8 \times 10^5 \text{ M}^{-1}$	Aqueous medium	Colorimetric and fluorometric
2	New J. Chem., 2017, <b>41</b> , 10096	Pyrazoline-based	7.56 mM for 4a, and 4.87 mM		HEPES/D MF	Colorimetric and fluorometric
3	RSC Adv., 2015, <b>5</b> , 91863	BODIPY - based	6.4 $\mu\text{M}$		Aqueous medium	Colorimetric and fluorometric
4	Sens. Actuators B Chem., <b>231</b> (2016) 752–758	Naphthofluorescein-based	1.74 M.		DMSO-PBS buffer	Colorimetric and fluorometric
5	Org. Biomol. Chem., 2014, <b>12</b> , 4637	Coumarin-quinolinium based	$8.9 \times 10^{-8} \text{ M}$		PBS buffer	Colorimetric and fluorometric
6	J. Agric. Food Chem. 2011, <b>59</b> , 11935–11939	Boron-dipyrromethene-based	$5.8 \times 10^{-5} \text{ M}$		$\text{H}_2\text{O}/\text{DMSO}$ solution (1:1)	Colorimetric and fluorometric
7	Chem. Commun., 2020, <b>56</b> , 10549	Fluorescein based	2.98 mM.		$\text{CH}_3\text{CN}/\text{PBS}$ buffer = 1/1,	Fluorometric

### References

1. D. Prabha, D. Singh, P. Kumar and R. Gupta, Inorg. Chem., 2021, **60**, 17889-17899.
2. N. Tripathi, P. Singh and S. Kumar, New J. Chem., 2017, **41**, 8739-8747.
3. S. Hussain, A. H. Malik, M. A. Afroz and P. K. Iyer, Chem. Commun., 2015, **51**, 7207-7210.